



The role of cluster mass in the multiple populations of Galactic and extragalactic Globular Clusters

Lagioia E. P. et al. 2019

Astronomical Journal, 158:202

Interpretation: Mixing or Primordial Abundance Variations?

EVIDENCE FOR MIXING It is hard to avoid the conclusion that globular cluster giants mix the ashes of internal nuclear processing to the surface on a scale larger than expected on the basis of classical evolutionary theory. The existence of CH and Ba stars in late evolutionary stages in clusters in

© Annual Reviews Inc. • Provided by the NASA Astrophysics Data System

332 KRAFT

which the vast majority of stars show no *generally* strong enhancement of carbon or s-process species suggests the correctness of the mixing hypothesis. CH stars seem to require that carbon produced by triple- α processing be mixed to the surface either at the He-core or shell flashes and the presence of Ba-stars in clusters suggests that the convective linkage necessary to operate the neutron-source chain $^{12}\text{C}(p, \gamma)^{13}\text{N}(\beta^+ \nu)^{13}\text{C}(\alpha, n)^{16}\text{O}$ in low mass stars must indeed exist.

In typical metal-poor cluster stars, as early as the mid-SGB, the average carbon abundance begins to decline presumably in response to the processing of the base of the convective envelope through the CN cycle, and continues to drop to ~ 0.1 of the original value, or lower, with advancing evolutionary state. The onset of the decline thus occurs much earlier and the magnitude of the effect is much larger than we would have expected based on the degree of CN processing and mixing found in conventional evolutionary models. Unfortunately, even with the improved observational technology cited earlier, it is not yet possible to recover the expected changes in the $^{12}\text{C}/^{13}\text{C}$ ratio in these stars. The lack of anti-

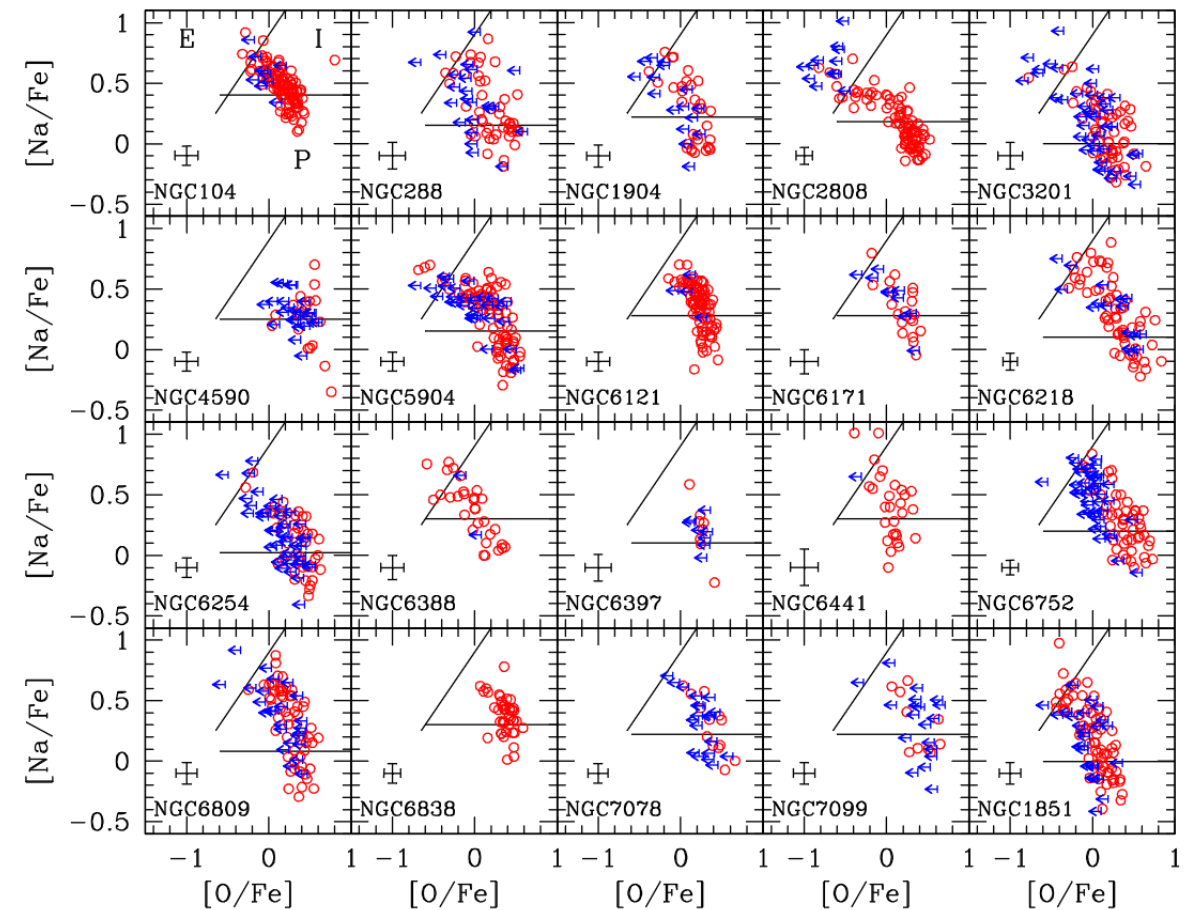
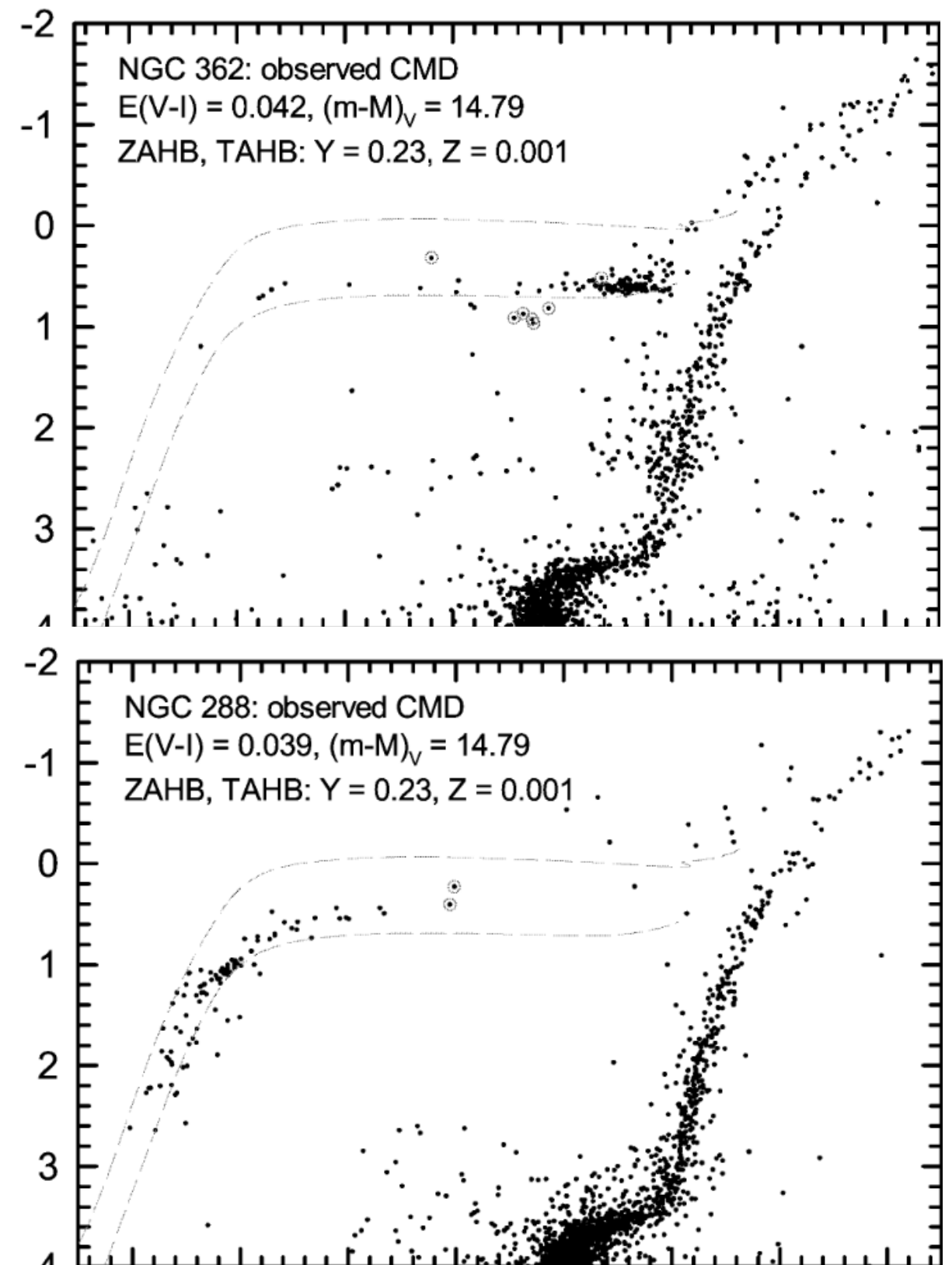
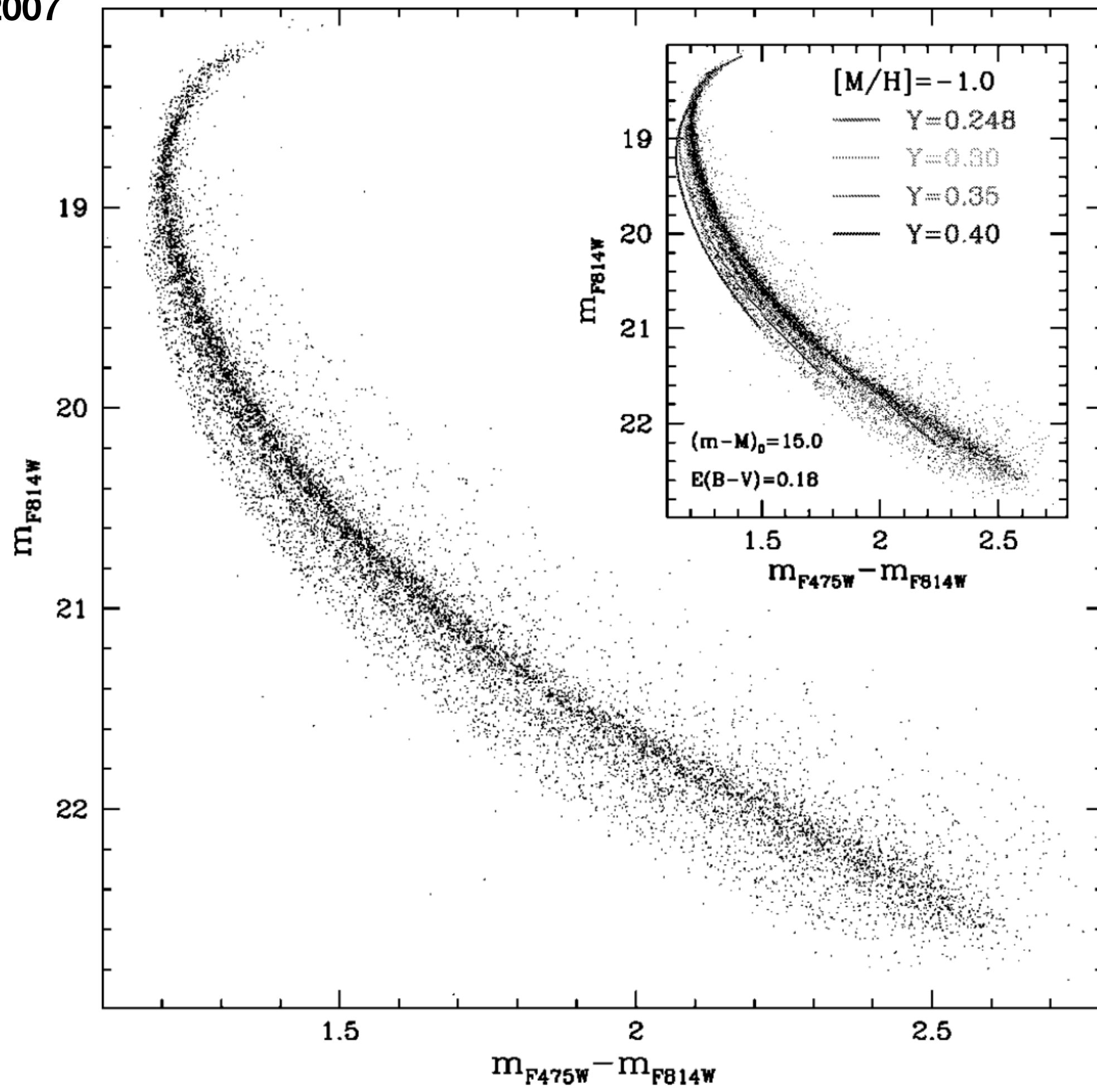


Fig. 2 A modern collection of Na-O anticorrelations showing partial results of the FLAMES survey of globular clusters (see Carretta et al. 2009a, 2010d for full references) and demonstrating both the ubiquity of this feature and its difference cluster-to-cluster. The lines separate the P (first generation), I, and E (second generation) components, as defined in Carretta et al. In this plot, red circles are measures for both O and Na, and blue arrows are measures for Na but only upper limits for O.

The "second"
parameter
of
HBs



Catelan+ 2001



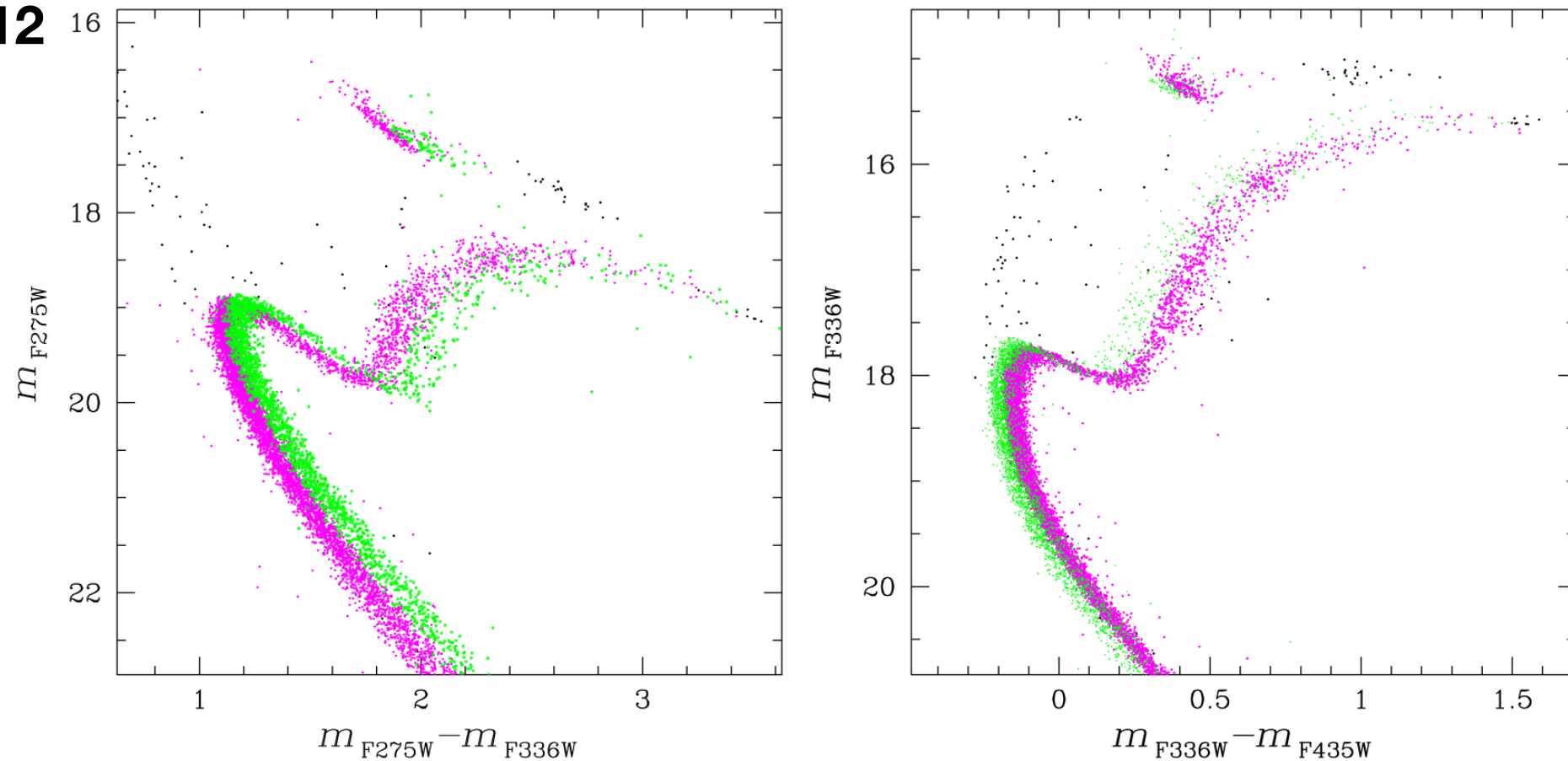


Figure 35. CMDs with m_{F275W} vs. $m_{F275W} - m_{F336W}$ (left) and m_{F336W} vs. $m_{F336W} - m_{F435W}$ (right). We have colored in green and magenta the two groups of stars selected in Figure 34. This is the first time anyone has been able to follow two stellar populations in a GC from the main sequence to the HB.

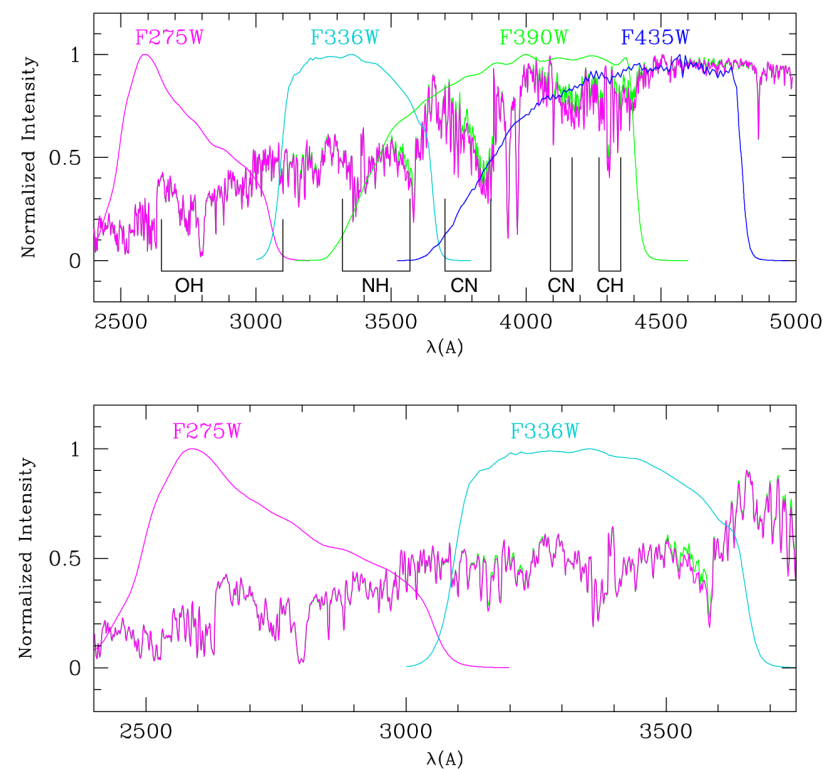
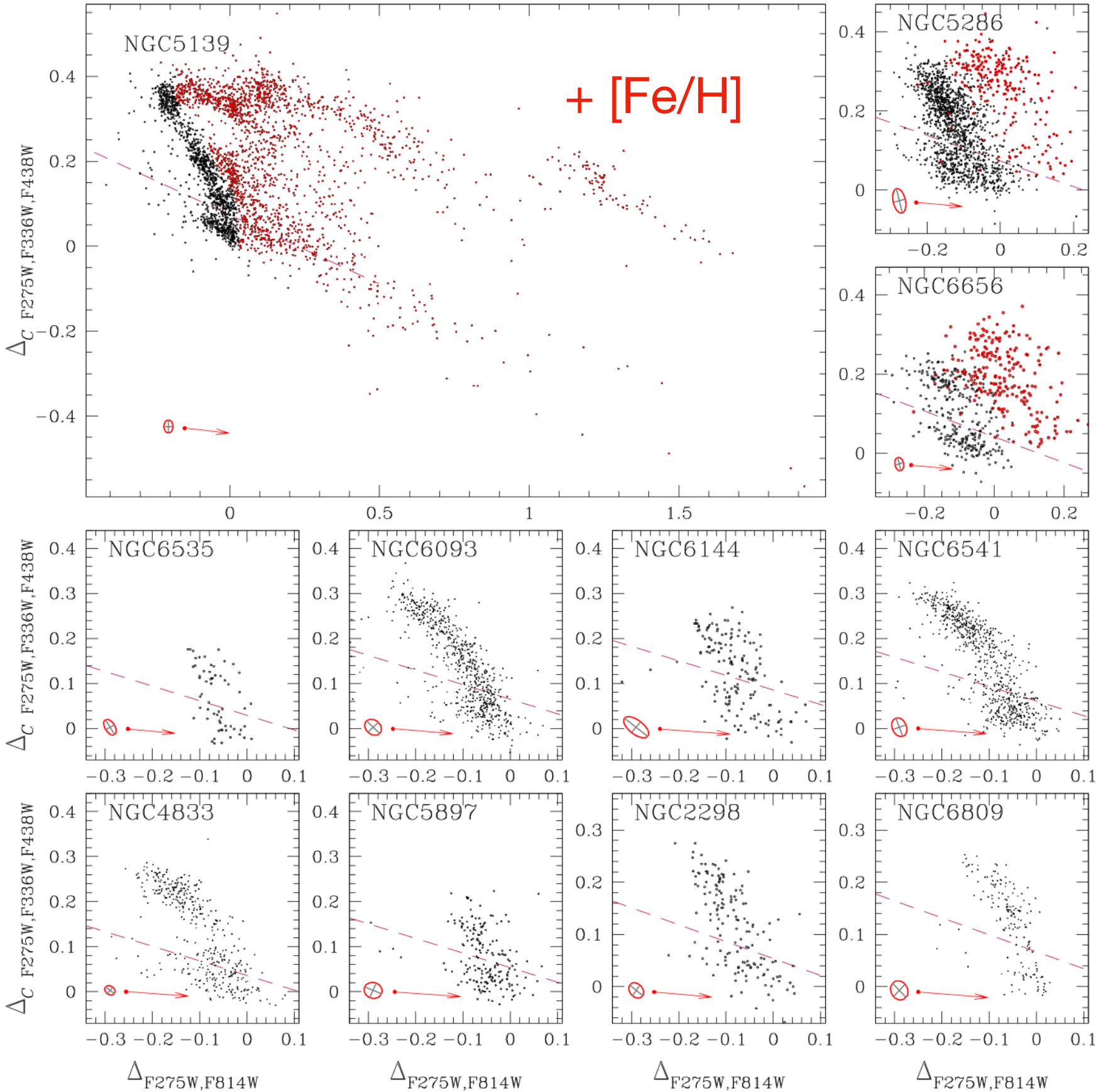


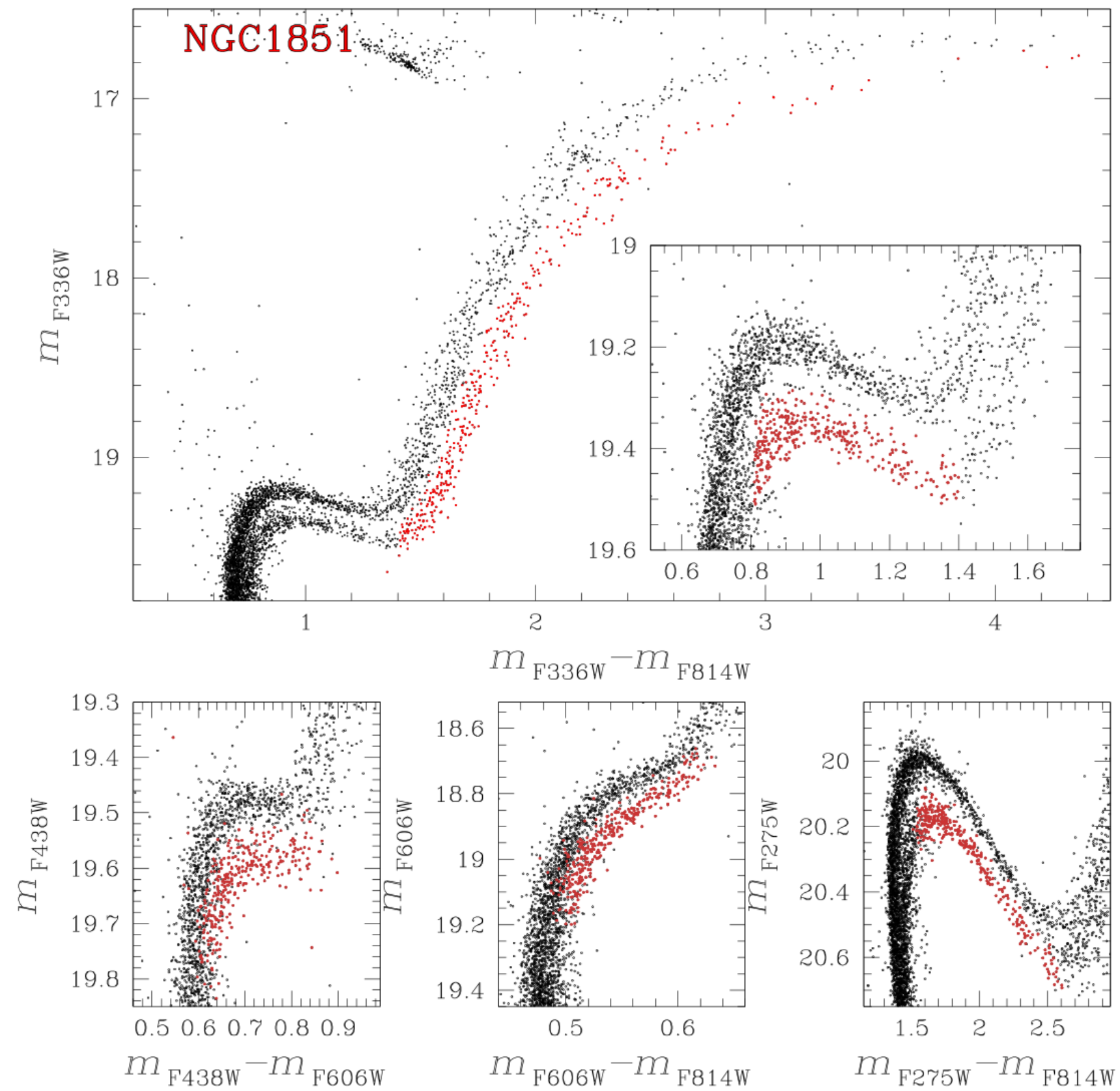
Figure 32. Top panel: comparison between two synthetic spectra: one for an N-rich star (magenta) and one for an N-poor star (black). The spectra are given as flux (in arbitrary units) and are smoothed at 1 Å resolution for clarity; they have been computed for parameters typical of a subgiant star in 47 Tuc, with chemical compositions given in the text. For reference, the normalized throughputs of the bluest broadband filters of WFC3/UVIS F(275/336/390/435/475)W are also shown. Labels on the bottom indicate the wavelength range where important spectroscopic features involving CNO elements cause significant absorption. The most important contributions come from OH at $\sim 2600\text{--}3100$ Å and NH at $\sim 3300\text{--}3600$ Å. Bottom panel: a zoom-in of the spectral region that is of particular interest for the present paper.

CNO variations mapped
through a specific combination
of UV and optical/NIR bands

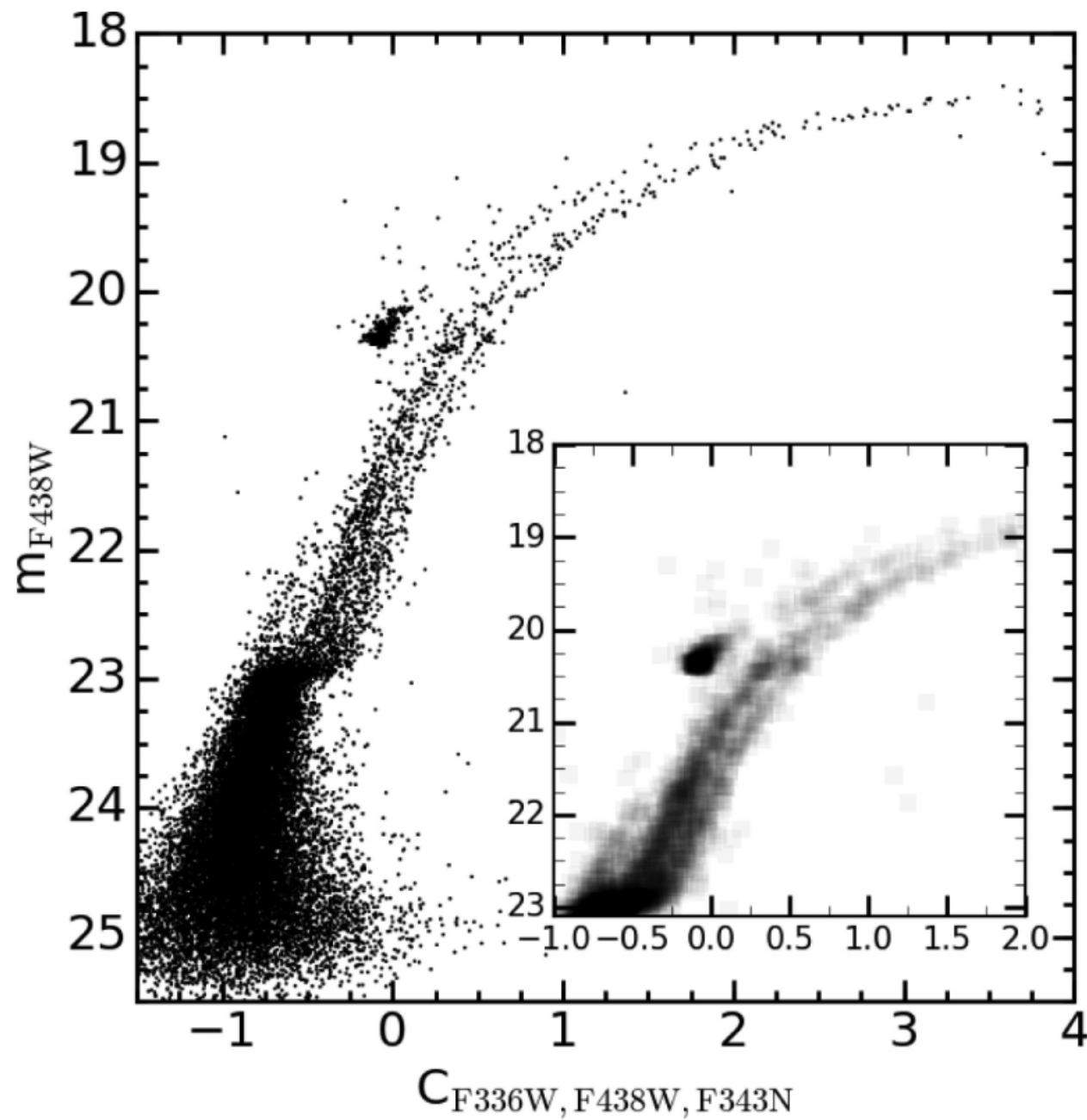


+ [Fe/H]

Type II GCs

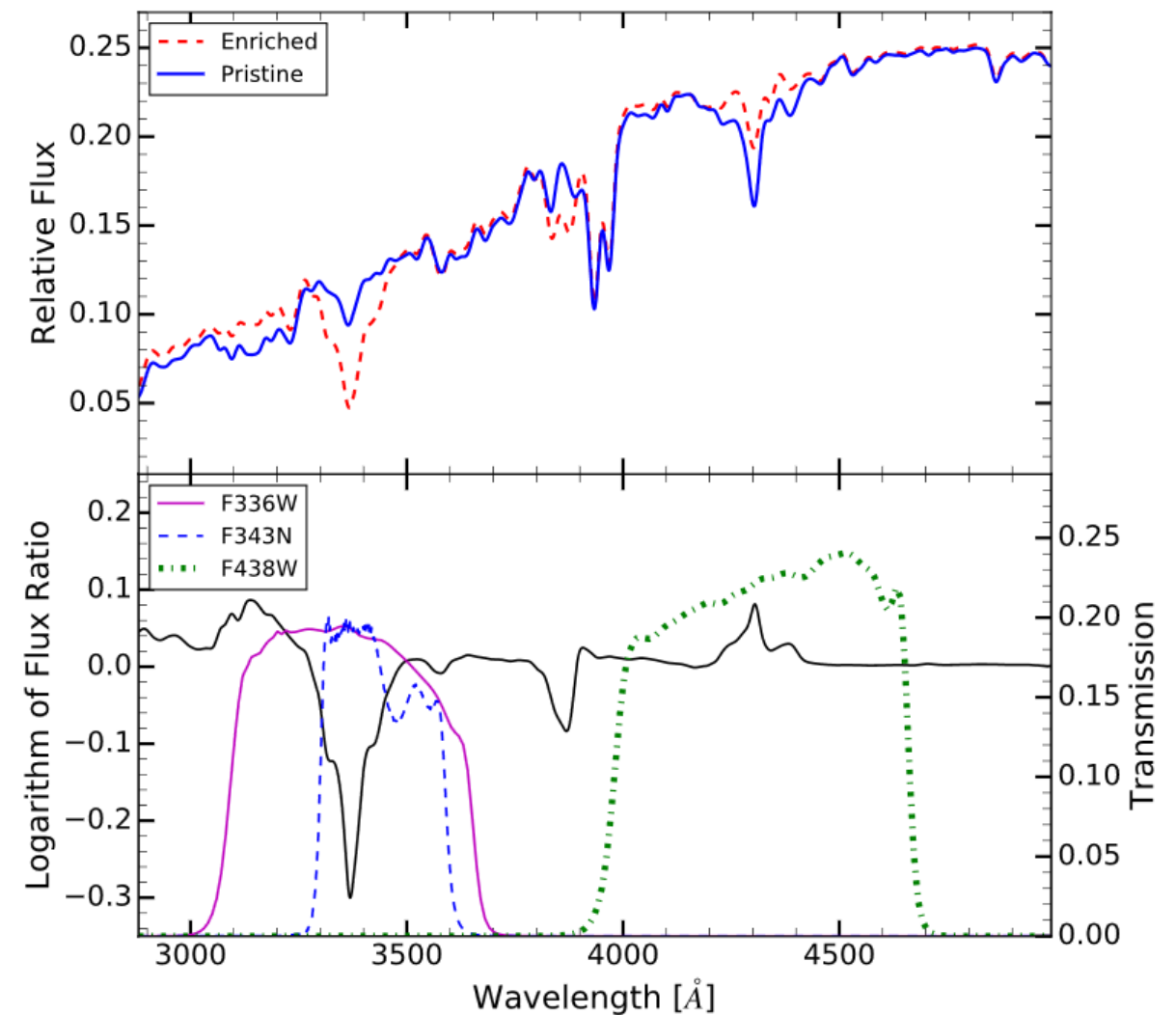


Milone+ 2017

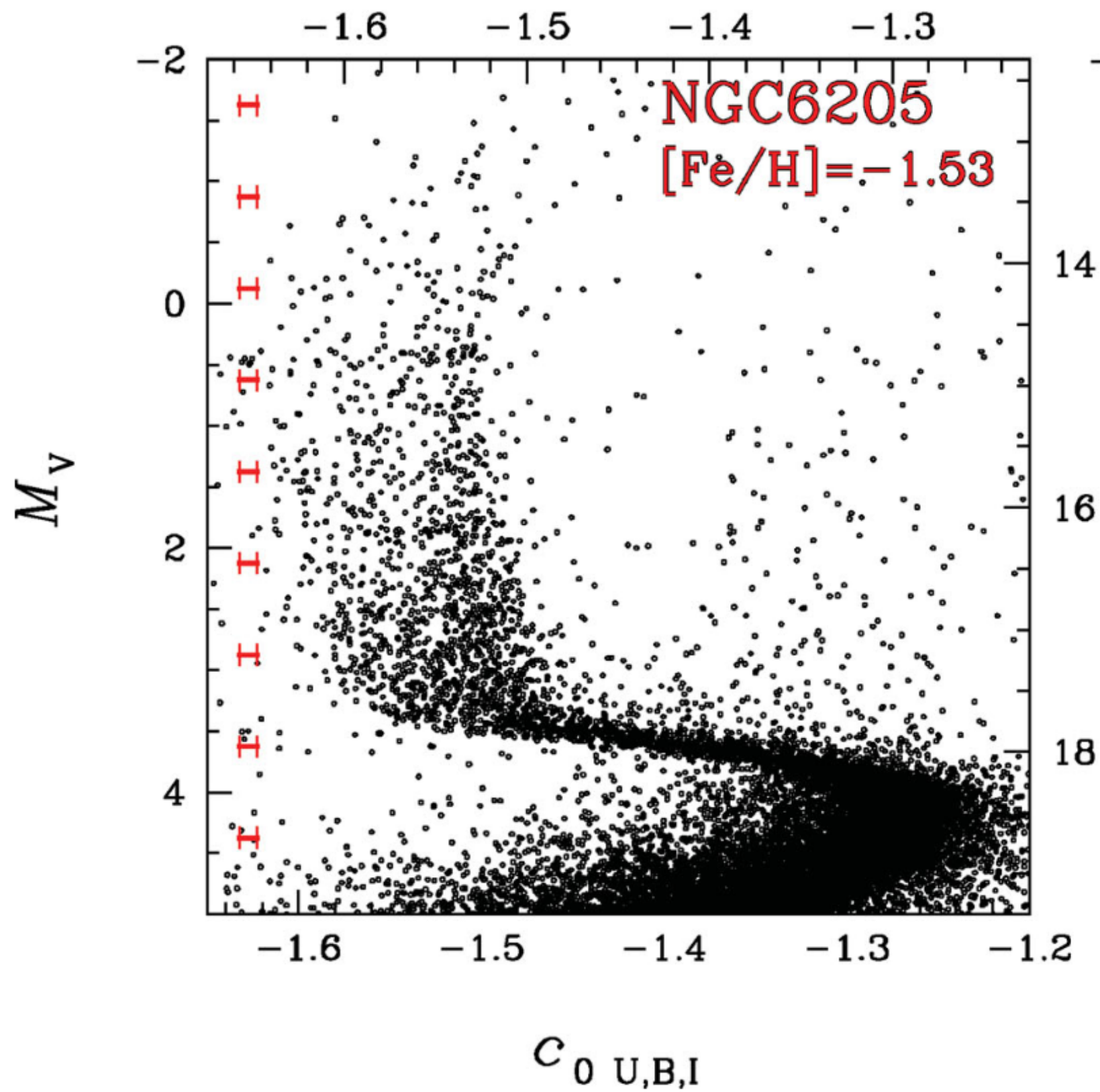


Niederhofer+ 2017

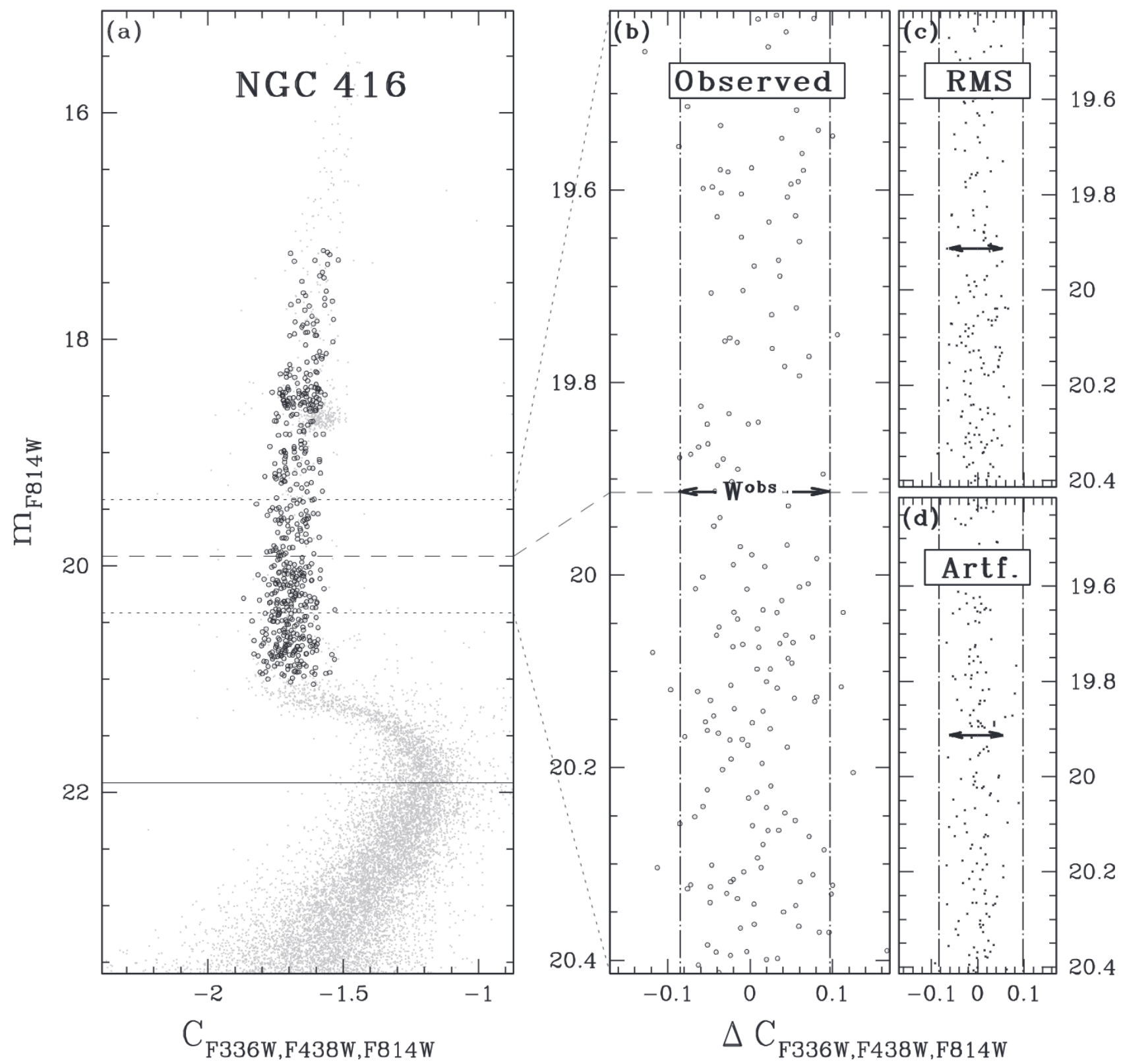
Old globular clusters
in the Magellanic clouds
also contain MSPs

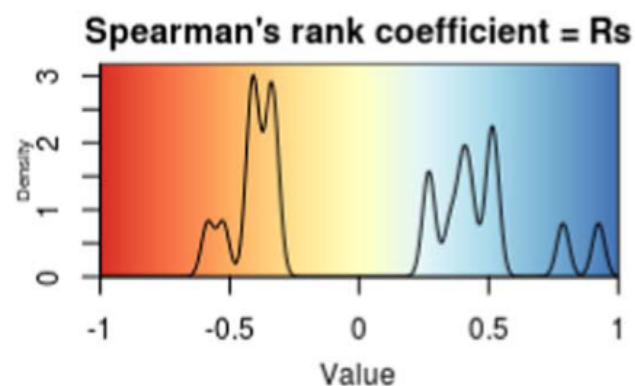


MSPs with ground-based photometry



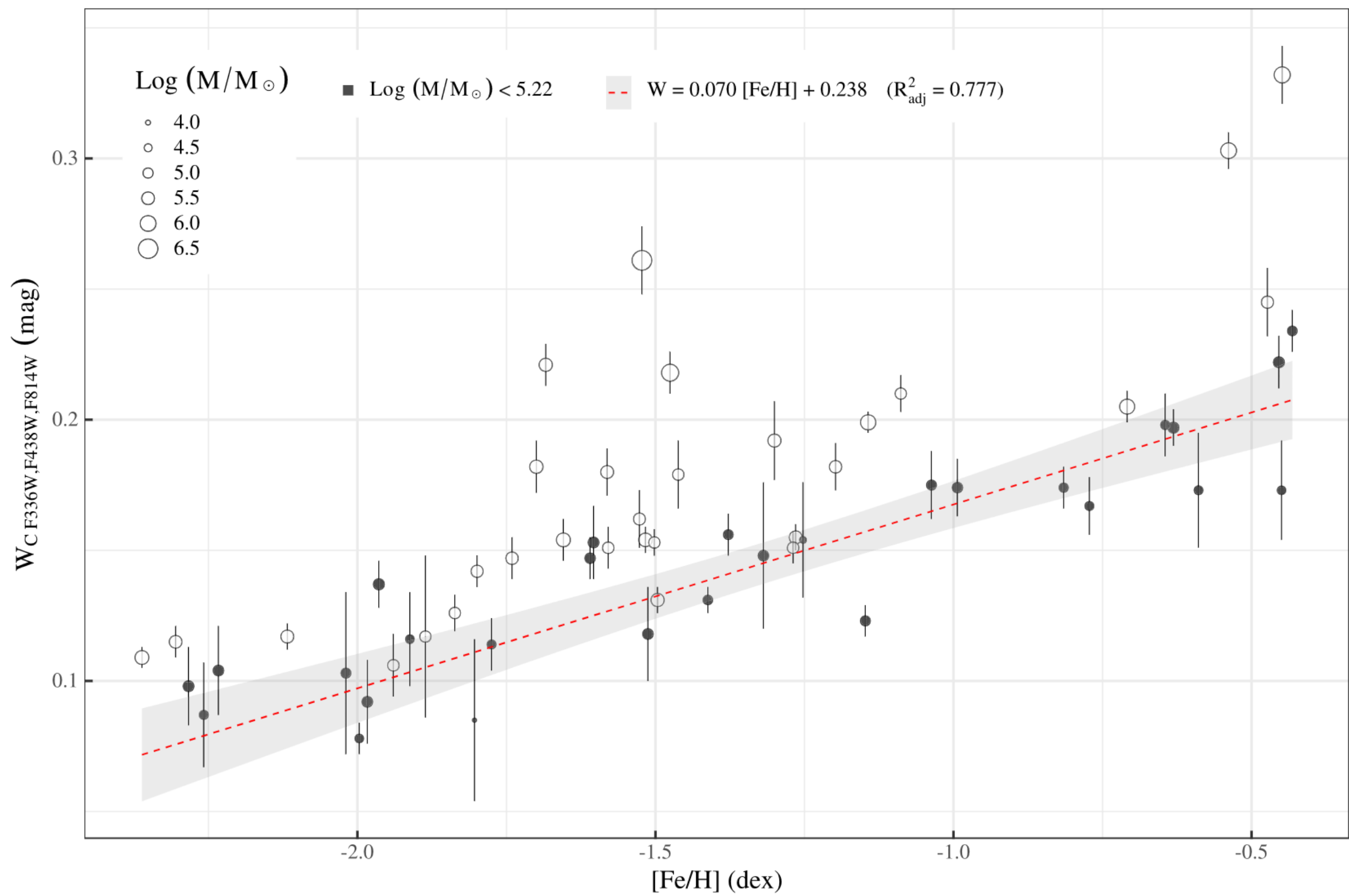
The RGB width

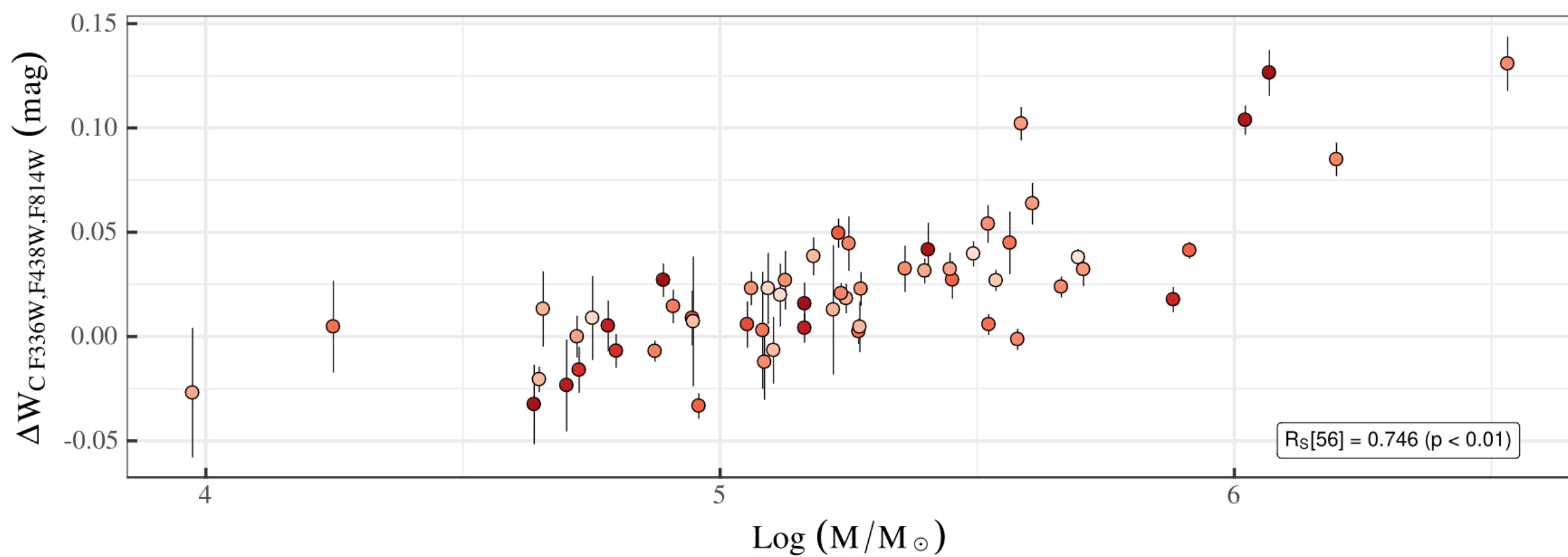
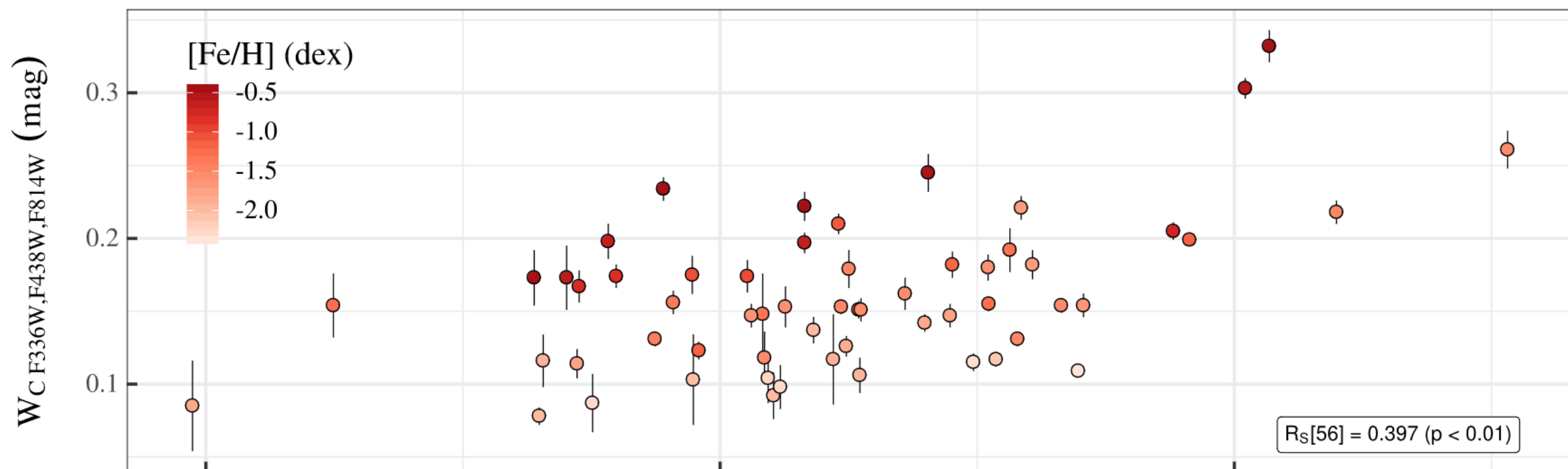


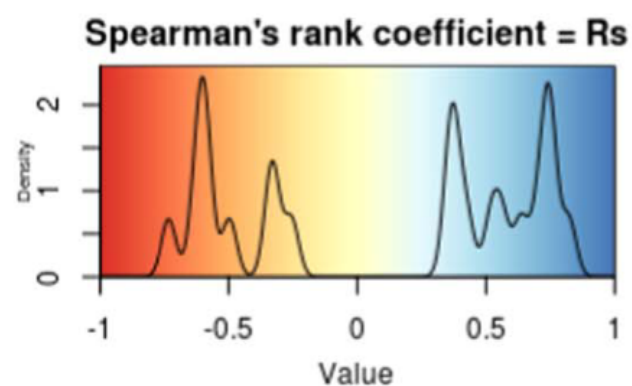


Correlation map of RGB Width against 45 GC parameters

[Fe/H]	epsilon	r_hl	T_rh	eta_c	Z	R_perig	<dY>	F_bin(c)
0.787 (56) <0.01	-0.038 (54) 0.78	-0.245 (56) 0.06	-0.092 (56) 0.49	-0.123 (56) 0.36	-0.131 (56) 0.33	-0.204 (56) 0.12	0.197 (55) 0.14	0.108 (34) 0.53
E(B-V)	c	r_hm	MF slope	eta_hm	U	R_apog	dY_max	F_bin(hm)
0.352 (56) 0.01	0.172 (56) 0.20	-0.337 (56) 0.01	0.266 (56) 0.04	0.172 (56) 0.20	0.055 (56) 0.68	-0.322 (56) 0.01	0.436 (55) <0.01	-0.135 (45) 0.36
Mv	Mass	r_t	F_remn	<RV>	V	age_MF09	W_C (M17)	F_bin(o-hm)
-0.420 (56) <0.01	0.397 (56) <0.01	-0.017 (56) 0.90	0.231 (56) 0.08	0.005 (56) 0.97	0.079 (56) 0.55	-0.071 (54) 0.60	0.924 (56) <0.01	-0.335 (41) 0.03
SB_0	M/L	rho_c	sigma_0	X	W	age_D10	N_1G/N_tot	HBR
-0.411 (56) <0.01	-0.040 (56) 0.77	0.273 (56) 0.04	0.513 (56) <0.01	-0.197 (56) 0.14	-0.073 (56) 0.58	-0.395 (56) <0.01	-0.416 (52) <0.01	-0.586 (55) <0.01
rho_0	r_c	rho_hm	v_esc	Y	R_GC	age_V13	S(RR Lyr)	L2
0.408 (56) <0.01	-0.180 (56) 0.18	0.525 (56) <0.01	0.505 (56) <0.01	-0.150 (56) 0.26	-0.354 (56) 0.01	-0.526 (49) <0.01	-0.192 (55) 0.15	0.181 (55) 0.18

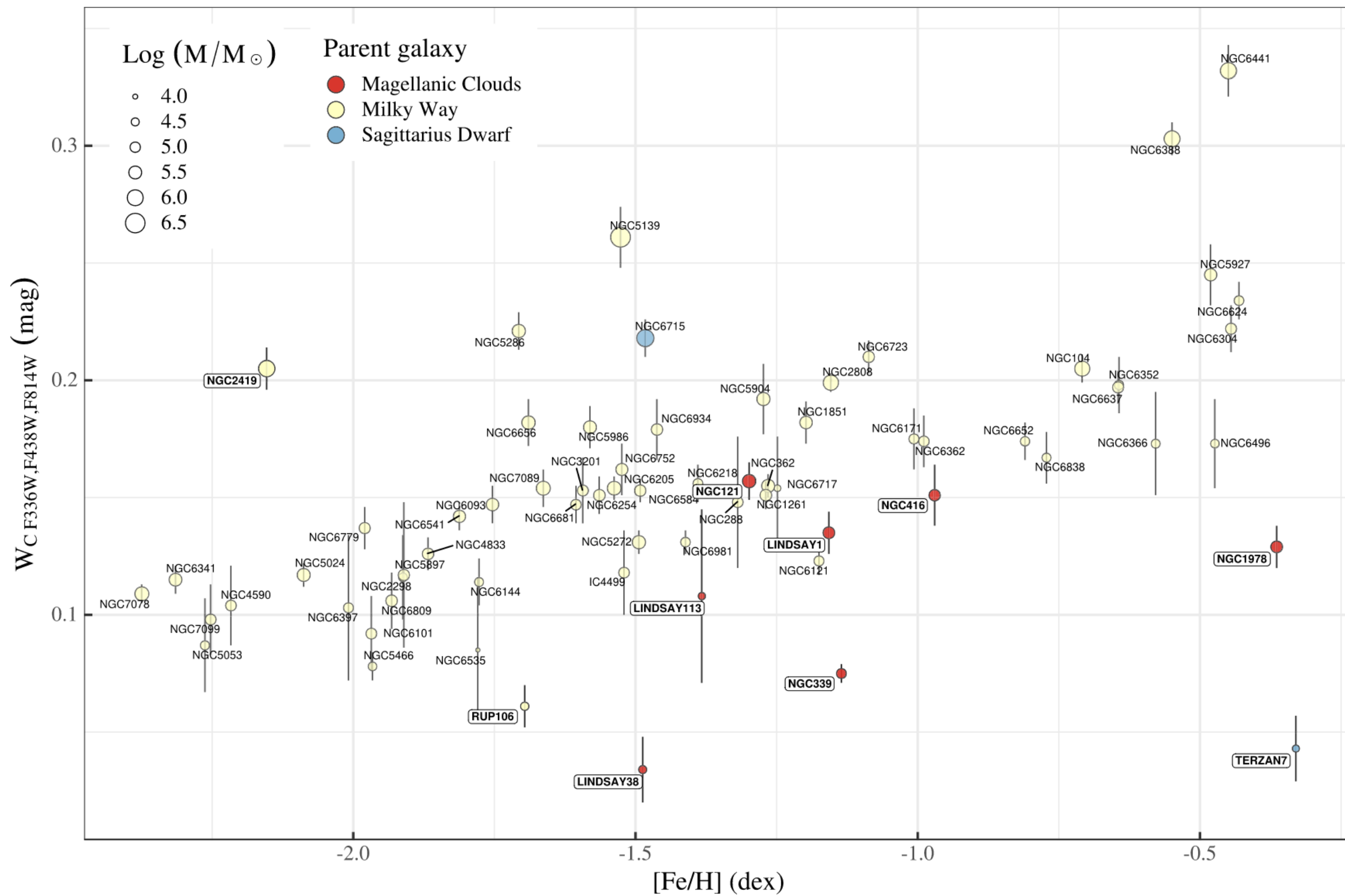


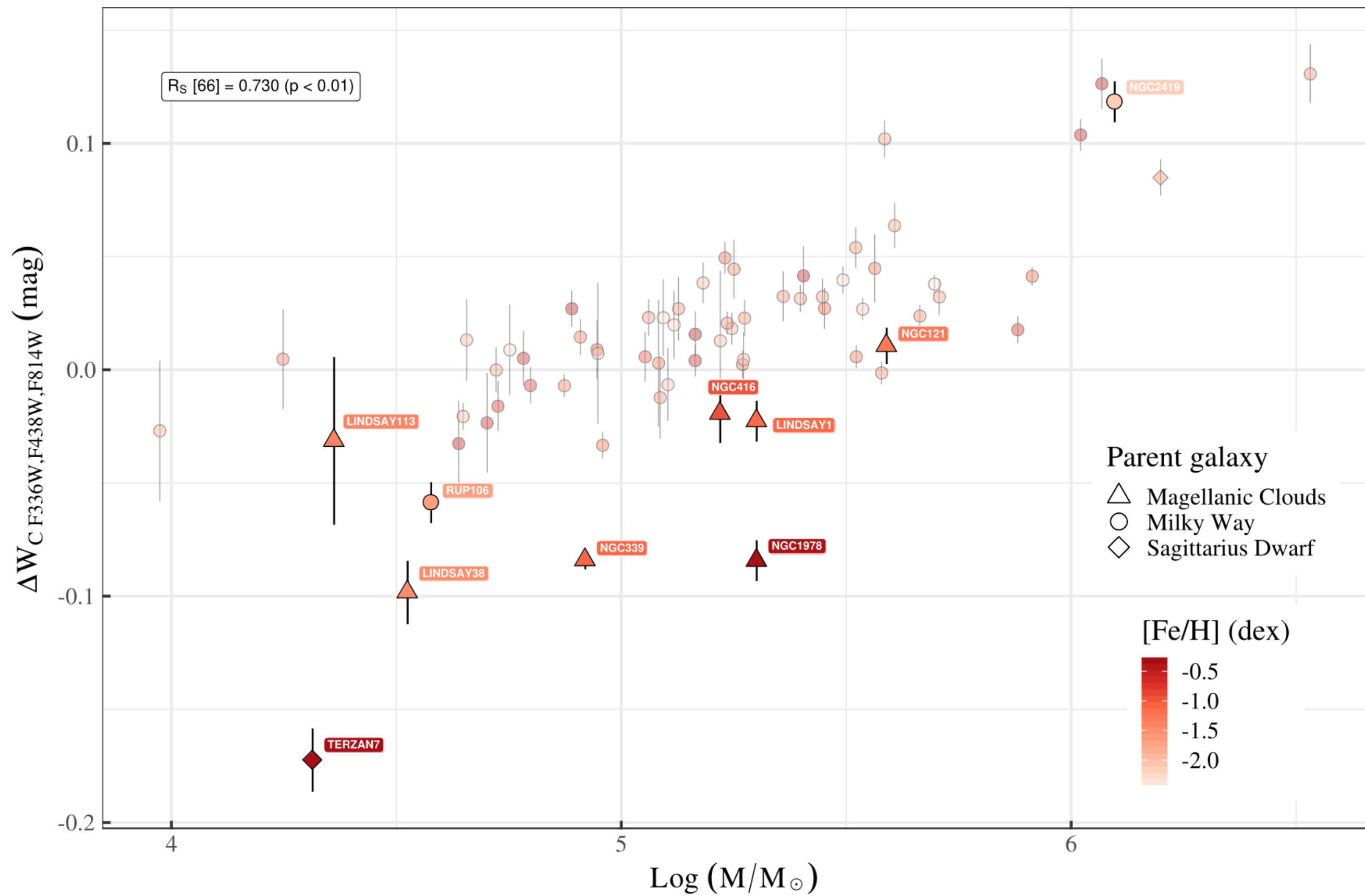


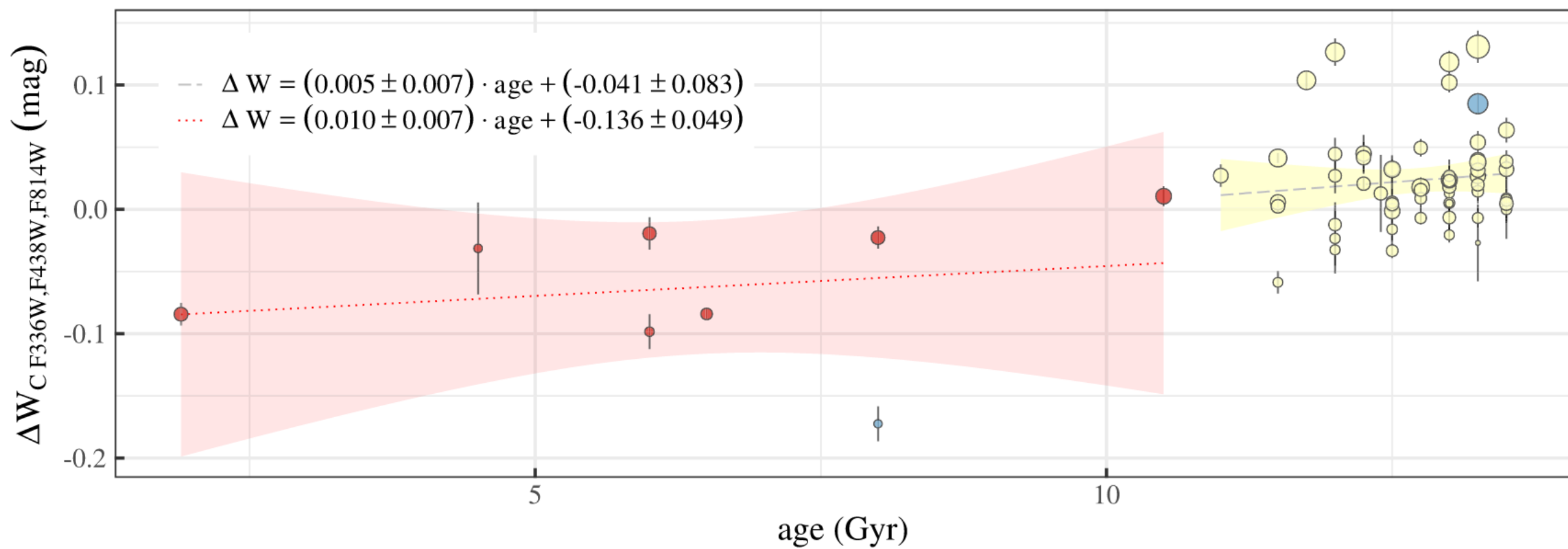
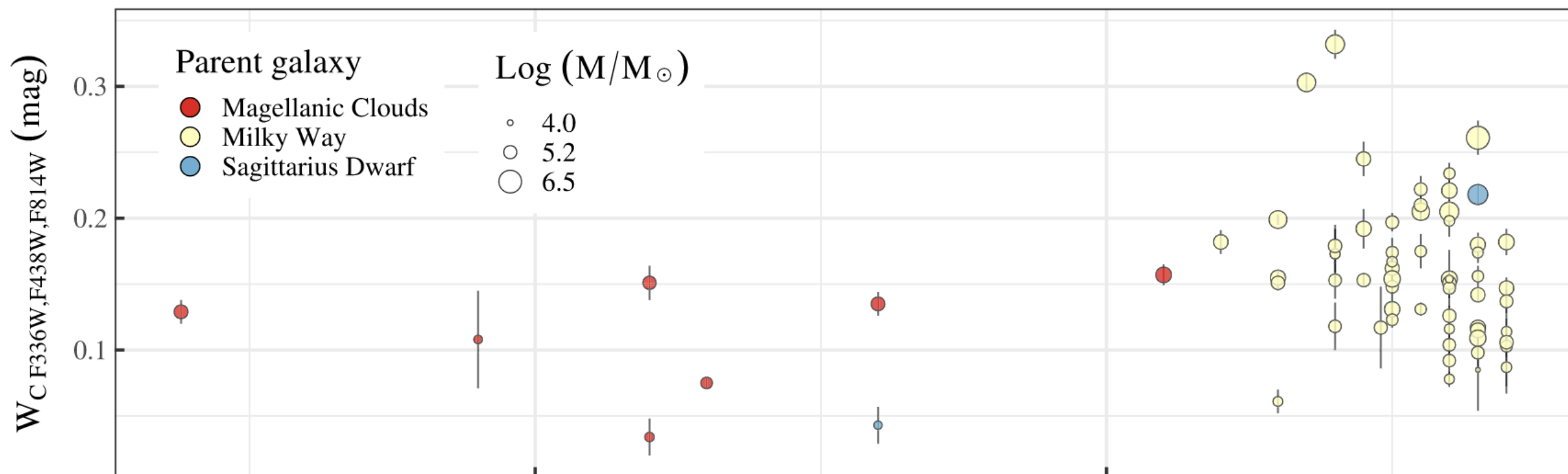


Correlation map of 'normalized' RGB Width against 44 GC parameters

	epsilon	r_hl	T_rh	eta_c	Z	R_perig	<dY>	F_bin(c)
	-0.020 (54) 0.88	-0.334 (56) 0.01	0.162 (56) 0.22	-0.256 (56) 0.05	0.082 (56) 0.54	-0.137 (56) 0.30	0.357 (55) 0.01	-0.497 (34) <0.01
E(B-V)	c	r_hm	MF slope	eta_hm	U	R_apog	dY_max	F_bin(hm)
0.080 (56) 0.55	0.376 (56) <0.01	-0.327 (56) 0.01	-0.220 (56) 0.10	0.047 (56) 0.72	-0.096 (56) 0.48	-0.006 (56) 0.96	0.703 (55) <0.01	-0.589 (45) <0.01
Mv	Mass	r_t	F_remn	<RV>	V	age_MF09	DW_C (M17)	F_bin(o-hm)
-0.733 (56) <0.01	0.746 (56) <0.01	0.372 (56) <0.01	-0.183 (56) 0.17	0.059 (56) 0.66	0.070 (56) 0.60	-0.191 (54) 0.16	0.822 (56) <0.01	-0.628 (41) <0.01
SB_0	M/L	rho_c	sigma_0	X	W	age_D10	N_1G/N_tot	HBR
-0.606 (56) <0.01	0.027 (56) 0.84	0.426 (56) <0.01	0.749 (56) <0.01	-0.094 (56) 0.48	-0.126 (56) 0.35	0.079 (56) 0.56	-0.591 (52) <0.01	0.044 (55) 0.74
rho_0	r_c	rho_hm	v_esc	Y	R_GC	age_V13	S(RR Lyr)	L2
0.520 (56) <0.01	-0.232 (56) 0.08	0.636 (56) <0.01	0.743 (56) <0.01	-0.054 (56) 0.69	-0.026 (56) 0.85	0.182 (49) 0.20	0.062 (55) 0.65	0.562 (55) <0.01







Conclusions

- for 68 GCs, measure of color extension of the stars at the base of the RGB in the UV–optical pseudocolor $C_{F336W,F438W,F814W}$ (sensitive to the stellar content of C, N, O, and helium)
- in the $W_{CF336W,F438W,F814W}$ versus $[Fe/H]$, young and intermediate-age MC clusters and Terzan 7 attain systematically lower RGB width values with respect to the MW GCs
- Rup 106 (mono stellar population) -> Terzan 7 likely a single population cluster
- comparison between the normalized RGB width of the MW and extragalactic GCs as a function of the cluster mass demonstrates that the extragalactic GCs systematically deviate
- comparison between the bulk trend of the Galactic GCs and the extragalactic systems shows that the latter attaining lower values of $DW_{CF336W, F438W, F814W}$ -> MC GCs exhibit smaller internal light-element variations than Galactic GCs with similar present-day masses
- does the observed difference depend on specific physical conditions in Galactic and extragalactic proto-GCs at the epoch of formation? or do MPs in MW and extragalactic GCs follow a unique trend with the initial cluster mass, but ancient Galactic GCs lost significant amount of their mass?

Your personal research assistant

Zotero is a free, easy-to-use tool to help you collect, organize, annotate, cite, and share research.

Download

Available for Mac, Windows, Linux, and iOS

Just need to create a quick bibliography? Try [ZoteroBib](#).

The screenshot displays the Zotero desktop application interface. The top window shows a search for 'Guerre, maladie, empire. Les services de santé militaires en ...' by Zaugg, 2016. Below this, a larger window shows a list of astronomy papers. The left sidebar shows a library structure with folders like 'My Library', 'Book Reviews', 'Colonial Medicine', 'Dissertation', 'Science and Empire', 'Teaching', 'Mapping', 'Open Access', 'Text Mining', and 'Visualization'. The main window lists papers with columns for Title, Citation Key, and a list of authors. The right sidebar shows details for a selected paper: 'Marino_2019_The_Hubble_Space_Telescope_UV_Legacy_Survey_of_Gal...' with a link to the article, filename, access date, pages, modified date, and indexed status.

Title	Creator	Year
Guerre, maladie, empire. Les services de santé militaires en ...	Zaugg	2016

Title	Citation Key
Different Stellar Rotations in the Two Main Sequences of the Young Globular Cluster NGC 1818: The First Dire...	marino18b
The Hubble Space Telescope UV Legacy Survey of Galactic Globular Clusters - XIX. A chemical tagging of the ...	marino19
Marino_2019_The_Hubble_Space_Telescope_UV_Legacy_Survey_of_Galactic_Globular_Clusters_-_pdf	marino19
Chemical Abundances along the 1G Sequence of the Chromosome Maps: The Globular Cluster NGC 3201	marino19a
Building the Galactic halo from globular clusters: evidence from chemically unusual red giants	martell11a
Age as a major factor in the onset of multiple populations in stellar clusters	martocchia18
The search for multiple populations in Magellanic Cloud clusters - IV. Coeval multiple stellar populations in th...	martocchia18a
The search for multiple populations in Magellanic Cloud clusters - V. Correlation between cluster age and ab...	martocchia19
Ceci N'est Pas a Globular Cluster: The Metallicity Distribution of the Stellar System Terzan 5	massari14b
GeMS MCAO observations of the Galactic globular cluster NGC 2808: the absolute age	massari16
Origin of the system of globular clusters in the Milky Way	massari19
Homogeneous analysis of globular clusters from the APOGEE survey with the BACCHUS code. I. The northern ...	masseron19
Full spectrum of turbulence convective mixing. II. Lithium production in AGB stars	mazzitelli99
Resolved Massive Star Clusters in the Milky Way and Its Satellites: Brightness Profiles and a Catalog of Funda...	mclaughlin05
Multiple stellar populations in Magellanic Cloud clusters. I. An ordinary feature for intermediate age globulars...	milone09
The radial distribution of the two stellar populations in NGC 1851	milone09a
Multiple Stellar Populations in the Galactic Globular Cluster NGC 6752	milone10
Luminosity and mass functions of the three main sequences of the globular cluster NGC 2808	milone12
Multiple Stellar Populations in 47 Tucanae	milone12a
Milone_2012_Multiple_Stellar_Populations_in_47_Tucanae.pdf	milone12b
A Double Main Sequence in the Globular Cluster NGC 6397	milone12c
The ACS survey of Galactic globular clusters. XII. Photometric binaries along the main sequence	milone12c
The Infrared Eye of the Wide-Field Camera 3 on the Hubble Space Telescope Reveals Multiple Main Sequences...	milone12d
A WFC3/HST View of the Three Stellar Populations in the Globular Cluster NGC 6752	milone13
Multiple stellar populations in Magellanic Cloud clusters. II. Evidence also in the young NGC 1844?	milone13a
Global and Nonglobal Parameters of Horizontal-branch Morphology of Globular Clusters	milone14
The M 4 Core Project with HST - II. Multiple stellar populations at the bottom of the main sequence	milone14a
Helium and multiple populations in the massive globular cluster NGC 6266 (M 62)	milone15
The Hubble Space Telescope UV Legacy Survey of galactic globular clusters - II. The seven stellar populations ...	milone15a
The Hubble Space Telescope UV Legacy Survey of Galactic Globular Clusters. III. A Quintuple Stellar Populatio...	milone15b
Milone_2015_The_Hubble_Space_Telescope_UV_Legacy_Survey_of_Galactic_Globular_Clusters_III.pdf	milone15c
Multiple stellar populations in Magellanic Cloud clusters - III. The first evidence of an extended main sequence...	milone16
The binary populations of eight globular clusters in the outer halo of the Milky Way	milone16a
Multiple stellar populations in Magellanic Cloud clusters - IV. The double main sequence of the young cluster ...	milone17
The Hubble Space Telescope UV Legacy Survey of Galactic globular clusters - IX. The Atlas of multiple stellar p...	milone17
Milone_2017_The_Hubble_Space_Telescope_UV_Legacy_Survey_of_Galactic_globular_clusters_-_IX_.pdf	milone17a
Multiple stellar populations in Magellanic Cloud clusters - V. The split main sequence of the young cluster NG...	milone17b
The HST large programme on ω Centauri - I. Multiple stellar populations at the bottom of the main sequence ...	milone18
Multiple stellar populations in Magellanic Cloud clusters - VI. A survey of multiple sequences and Be stars in y...	milone18a
Gaia unveils the kinematics of multiple stellar populations in 47 Tucanae	milone18b
The Hubble Space Telescope UV legacy survey of galactic globular clusters - XVI. The helium abundance of mu...	milone19
Milone_2018_The_Hubble_Space_Telescope_UV_legacy_survey_of_galactic_globular_clusters_-_pdf	milone19
The HST Large Programme on NGC 6752 - II. Multiple populations at the bottom of the main sequence probed...	milone19

Marino_2019_The_Hubble_Space_Telescope_UV_Legacy_Survey_of_Gal...
<https://academic.oup.com/mnras/article-pdf/487/3/3815/28848619/stz1415...>
Filename: Marino_2019_The_Hubble_Space_Telescope_UV_Legacy_Survey_...
Accessed: 11/28/2019, 6:45:14 PM
Pages: 30
Modified: 11/28/2019, 6:45:15 PM
Indexed: Yes

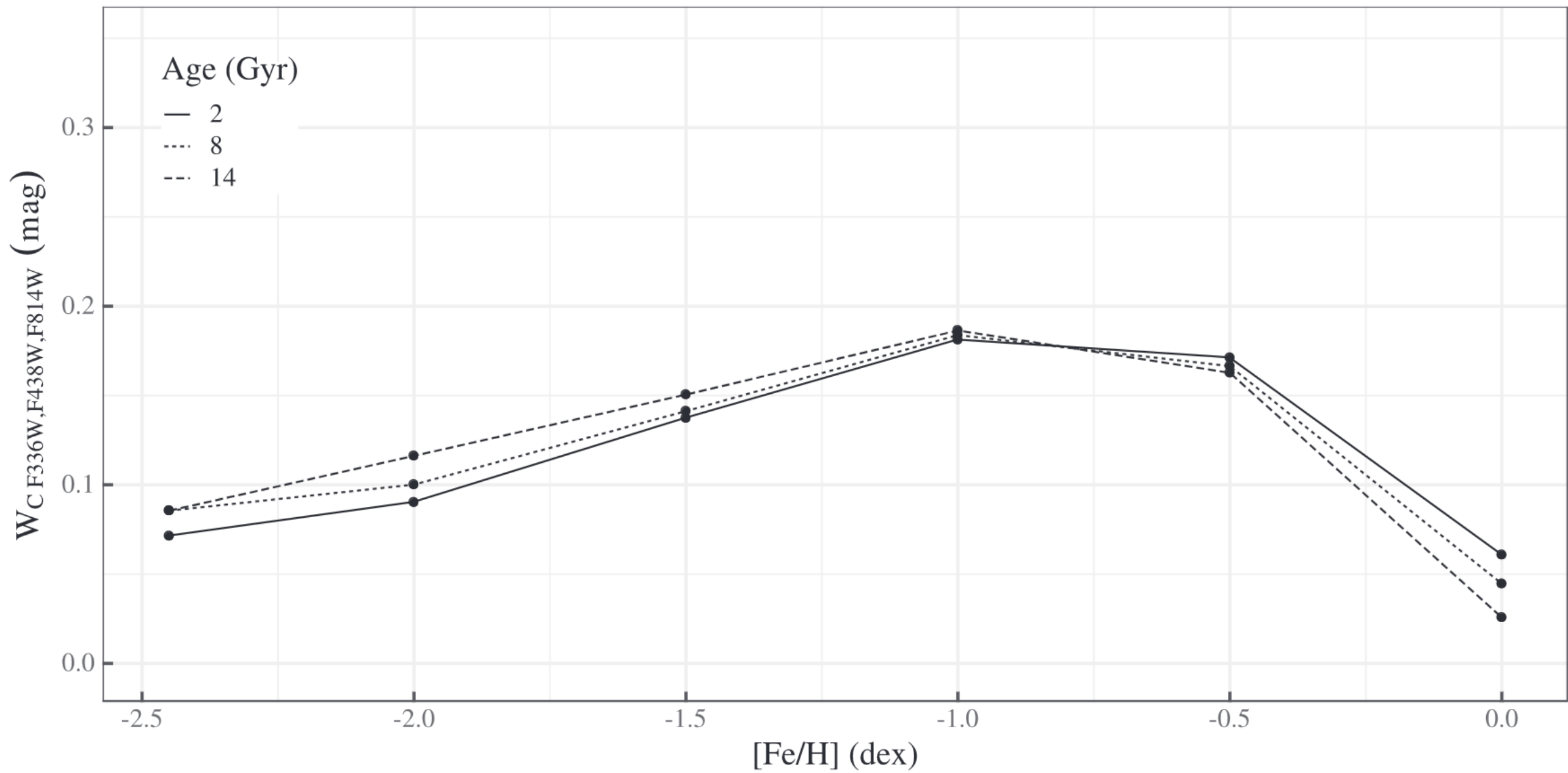


Figure 7. Theoretical variation of the RGB width as a function of metallicity $[\text{Fe}/\text{H}]$ for young, intermediate-age, and old models.